forests

MDPI

Article

Variation in Stem Xylem Traits is Related to Differentiation of Upper Limits of Tree Species along an Elevational Gradient

Da Yang [1,2], Ai-Ying Wang [1,3], Jiao-Lin Zhang [2], Corey J. A. Bradshaw [4] and Guang-You Hao [1,*]

1 CAS Key Laboratory of Forest Ecology and Management, Institute of Applied Ecology, Chinese Academy of Sciences, Shenyang, Liaoning 110010, China; yangda@xtbg.ac.cn (D.Y.); aiyingwqepq@163.com (A.-Y.W.)
2 CAS Key Laboratory of Tropical Forest Ecology, Xishuangbanna Tropical Botanical Garden, Chinese Academy of Sciences, Mengla, Yunnan 666303, China; zjl@xtbg.org.cn
3 School of Life Sciences and Engineering, Shenyang University, Shenyang, Liaoning 110044, China
4 Global Ecology, College of Science and Engineering, GPO Box 2100, Flinders University, Adelaide, SA 5001, Australia; corey.bradshaw@flinders.edu.au
* Correspondence: haogy@iae.ac.cn; Tel.: +86-24-83970374

Received: 3 December 2019; Accepted: 16 March 2020; Published: 20 March 2020

Abstract: The distribution limits of many plants are dictated by environmental conditions and species' functional traits. While many studies have evaluated how plant distribution is driven by environmental conditions, there are not many studies investigating xylem vessel properties with altitude, and whether these traits correlate with altitudinal distribution of tree. Here, we investigated the upper limits of distribution for ten deciduous broadleaf tree species from three temperate montane forest communities along a large elevational gradient on the north-facing slope of Changbai Mountain in Northeast China. We measured stem xylem traits associated with a species' ability to transport water and resist freezing-induced cavitation that theoretically represent important adaptations to changes in climatic conditions along the elevational gradient. Hydraulically weighted vessel diameter (D_h) was negatively correlated with with the upper limit across the ten studied tree species; however, the correlation seems to be driven by the large differences between ring- and diffuse-porous tree species groups. The ring-porous tree species (e.g., *Fraxinus mandshurica* Rupr., *Maackia amurensis* Rupr. et Maxim., and *Phellodendron amurense* Rupr.) had considerably wider vessels than the diffuse-porous species and were all limited to low-elevation communities. The coefficient of variation (CV) for D_h was 0.53 among the 10 studied species, while the intraspecific analysis showed that the highest CV was only 0.22 among the 10 species. We found no evidence of a relationship between D_h and the upper limits across the seven diffuse-porous species. In contrast to elevation, hydraulic-related xylem traits had no clear patterns of change with precipitation, indicating that hydraulic functionality was largely decoupled from the influences of precipitation in the study area. This finding suggests that xylem traits are associated with altitudinal limits of species distribution, which is mostly evidenced by the contrasts between ring- and diffuse-porous species in xylem anatomy and their altitudinal distributions.

Keywords: elevation; freezing stress; functional traits; species distribution; xylem anatomy

1. Introduction

An understanding of what drives patterns of species distributions has long been a primary goal in ecology, including the ecophysiological mechanisms involved [1–3]. Generally, tolerance to abiotic stresses is a major determinant of species distributions, especially at extremes of temperature, water, and light availability [4–6]. Many ecophysiological studies have focused on species distributions across

broad geographic ranges and stress conditions [7,8], such as the relationship between distributions and water availability [9–11]. While there has been progress linking spatial distributions of species to environmental gradients using species distribution models [12,13], the physiological mechanisms underlying these mostly correlative patterns are seldom understood [10]. As a result, we generally lack a robust capacity to predict how plant distributions will shift with climate change.

Generally, climate has been recognized as an important factor determining species' geographic distributions [9,14]. For example, there is evidence that low winter temperatures determine species distributions along altitudinal or latitudinal gradients by inducing freezing injury to living tissues and harming the hydraulic function of xylem conduits by inducing embolisms [15]. It has also been found that the growing season length, temperatures or both constrain latitudinal and elevational range limits of plant species [16–18]. For instance, growing-season length constrained the upper limits of European plants along an elevational gradient [16]. Low growing-season temperatures can also determine the upper limits of elevational distributions in alpine tree species [17,19].

The distribution of trees along environmental gradients can be influenced by functional traits considered adaptive for local environmental conditions [20–23]. Measuring the most influential functional traits in this regard, therefore, offers a promising pathway to understanding and predicting how vegetation properties and species distributions are modified along geographical gradients [24–26]. There is evidence that physiological trait variation explains niche differentiation between *Betula* species along an altitudinal gradient [27]. Particularly, plant traits related to hydraulics are informative of functional strategies and hence species distributions in that they can be strongly affected by environmental stress such as freezing temperatures and drought [28–33]. Catastrophic embolism in conduit networks can diminish a plant's ability to transport water, reduce photosynthetic productivity, or even result in death [34,35]. As such, a plant's capacity to reduce the detrimental effects of embolism is an important adaptive trait for growth and survival in extreme temperature or -moisture environments [35–37]. For example, hydraulic traits help explain niche segregation in Mediterranean woody species along an aridity or elevational gradient [23]. Moreover, wood density is a functionally relevant traits that reflects safety in water transport because its variation is related to the vulnerability of xylem to cavitation and embolism [38,39].

We established an elevational transect in a temperate montane forest from the north-facing slope of the Changbai Mountain to provide insight into the influence of environmental variation along a steep temperature gradient [40]. We used this approach to test the coupled effects of the elevational gradient and variation in stem hydraulic-related traits on species distributions, with a focus on xylem anatomical characteristics related to freezing-induced xylem embolism in this high-mountain temperate forest ecosystem. Low winter temperatures and freeze/thaw events pose a great challenge to the physiology and survival of all temperate perennial plants, with the twigs or terminal branches of trees, in particular, frequently experiencing high stress during long and cold winters, especially at high elevations [41,42]. This is because xylem vessels in branches are vulnerable to embolism that reduces hydraulic efficiency induced by frequent freeze/thaw events [43]. Narrower vessels tend to be more resistant to freeze/thaw-induced embolism [44], so the conduit diameter of the xylem can be used as a proxy for resistance to freeze/thaw-induced embolism. We therefore hypothesized that tree species at higher elevations would have smaller vessel diameters than their lower-elevation counterparts to be able to resist lower temperatures and more frequent freeze/thaw events.

We examined the relationships between three relevant xylem traits (hydraulically weighted vessel diameter, xylem vessel density and sapwood density) and upper limits of the distribution of ten native temperate deciduous broadleaf tree species along the north-facing slope of Changbai Mountain in Northeast China (Table 1). We hypothesized that across this elevational gradient, stem xylem traits would vary in a manner consistent with the prediction of increasing hydraulic safety (smaller hydraulically weighted vessel diameter) with increasing elevation and decreasing temperature. We assessed whether variation in these functional traits related to xylem hydraulics underlies the upper distributional limits of tree species.

Table 1. Basic information of the 10 tree species examined. 'D' and 'R' represent diffuse-porous and ring-porous, respectively.

Species	Species Code	Family	Upper Limit (m)	Wood Type
Alnus japonica Sieb. et. Zucc.	AJ	Betulaceae	1500	D
Alnus mandshurica (Callier ex C. K. Schneider) Hand.	AM	Betulaceae	2000	D
Betula ermanii Cham.	BE	Betulaceae	2000	D
Betula platyphylla Suk.	BP	Betulaceae	1500	D
Fraxinus mandschurica Rupr.	FM	Oleaceae	1000	R
Maackia amurensis Rupr. et Maxim.	MA	Leguminosae	1000	R
Phellodendron amurense Rupr.	PA	Rutaceae	1000	R
Populus ussuriensis Kom.	PU	Salicaceae	1100	D
Sorbus pohuashanensis (Hance) Hedl.	SP	Rosaceae	1850	D
Tilia amurensis Rupr.	TA	Tiliaceae	1100	D

2. Materials and Methods

2.1. Study Area

Our study area was in Changbai Mountain National Reserve (42° 42–10′ N, 127° 38–10′ E) in Jilin Province, Northeast China. Changbai Mountain National Reserve was established in 1980 and is a typical and well-preserved mountainous forest ecosystem in China that contains a wide range of climate and vegetation types with distinct elevational distributions [45]. The sites we used are characterized by contrasting climatic conditions and forest communities along an elevational gradient (Figure 1). The region has a climate typical of a temperate, continental mountain monsoon ecosystem, with climate conditions varying widely as elevation increases. Annual precipitation ranges from 707 to 893 mm and mean annual temperature ranges from 3.25 °C at 735 m elevation to −1.83 °C at 2000 m elevation. A wet and warm growing season occurs from June to August, while a relatively dry and cold season occurs from September to May [46]. The mean storm (wind > 17 m s^{-1}) frequency ranges from 30 days $year^{-1}$ at 774 m to 267 days $year^{-1}$ at 2623 m [47]. Thus, we assume that the short duration of the summer monsoon and long, cold and dry winters are the main natural climatic conditions responsible for the distribution of these vegetation communities.

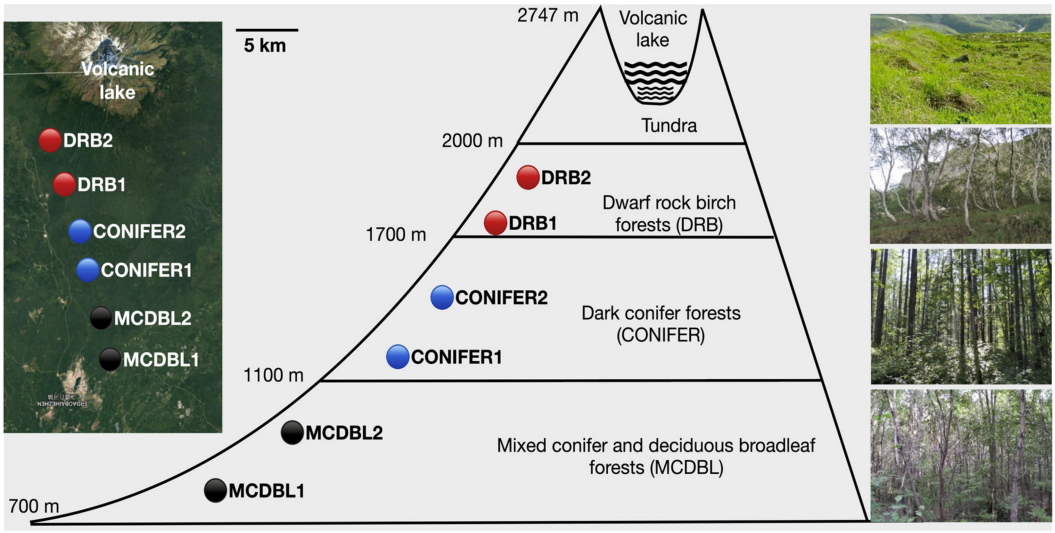

Figure 1. Diagram map of sampling sites from three forest types along elevations on the northern slope of Changbai Mountain in Northeast China.

Variation in climate with elevation leads to a vertical zonation from temperate mixed coniferous and broadleaf forest to alpine tundra, which is unique in China. There are four distinct vertical vegetation belts, including three major forest types at elevations < 2000 m and one alpine tundra

at elevations > 2000 m on the north-facing slope of Changbai Mountain. The three typical vertical forest belts of vegetation we selected are: (*i*) mixed conifer and deciduous broadleaf forests occupying areas between 700 and 1100 m (low elevation), (*ii*) conifer forests between 1100 and 1700 m (middle elevation), and (*iii*) dwarf rock birch forests between 1700 and 2000 m (high elevation) [48,49]. We set two sampling sites in each forest type: *deciduous broadleaf 1* and *2*, *conifer 1* and *2*, and *dwarf rock birch (DRB) 1* and *2* (Figure 1 and Table 2).

Table 2. The list of six sampling sites distributed in three forest types along the altitudinal gradient, showing the sampled species at each site. Species codes are given in Table 1. mixed conifer and deciduous broadleaf forests: MCB, dark conifer forests: CONIFER, dwarf rock birch forests: DRB. '+' refers to presence of that species.

Forest Type	Site		Species									
	Code	Elevation	FM	MA	PA	PU	TA	SP	BP	BE	AJ	AM
MCDBL	MCDBL1	735	+	+	+	+	+	+	+		+	
	MCDBL2	920	+	+	+	+	+	+	+		+	
CONIFER	CONIFER1	1150						+	+		+	
	CONIFER2	1400						+	+		+	
DRB	DRB1	1700						+		+		+
	DRB2	1850						+		+		+

2.2. Elevational Transect and Choices of Species

We established an elevational transect on the northern slope of Changbai Mountain, covering a wide range of environments of these three forest belts. The low elevation of the gradient comprised several deciduous broadleaf tree species (e.g., *Acer mono*, *Fraxinus mandshurica*, *Phellodendron amurense*, *Sorbus pohuashanensis*, *Tilia amurensis* and *T. mandshurica*) mixed with *Pinus koraiensis*. The vegetation at the lowest end of the gradient represents the typical low-elevation forest covering a broad region of Northeast China. The highest elevation of the gradient comprises relatively fewer tree species dominated by *Betula ermanii* and *Alnus mandshurica*. The site located at the highest end of the gradient (2000 m elevation) is near the alpine treeline. The forest vegetation near the alpine treeline resembles the forest vegetation located near the Arctic treeline in the Russian Far East in terms of forest structure and dominant species [40]. This elevational gradient is, therefore, ideal for investigating how coupling climate with functional trait variation drives the observed patterns in the upper limits of species distributions.

We identified ten target deciduous broadleaf tree species whose upper limits of distribution are mostly or entirely covered by our elevational transect, including seven diffuse-porous species and three species with a ring-porous wood (Table 1).

2.3. Sampling and Trait Measurements

We sampled target trees at the six elevational sites (two for each forest type, Table 2). We collected all data at each site during late June and early August of 2016. At each site, we randomly selected six mature individuals (diameter at breast height ranging from 10 to 20 cm) of each species that occurs in the specific site for stem and leaf sampling. To minimize the impact of sampling height (or variation within individuals) on plant functional traits, we took all samples from sun-exposed branches at heights 4–6 m above ground level.

We used six stem segments of 20 cm in length and 5-10 mm in diameter from six different individuals of each species from each site for the anatomical measurements. We used the mass of the water displaced by the wood sample (stem segments of 5 cm in length with bark removed) to calculate fresh volume. We then dried these wood samples at 60 °C for 72 h and determined the dry mass using a four-digit analytical balance (Sartorius model 222D balance, Sartorius Corp., Princeton, NJ, USA). We calculated sapwood density of stems (WD, g cm^{-3}) as dry mass divided by fresh volume. We cut the remaining part of each wood sample into 5-cm lengths to measure xylem vessel traits, cutting

the cross-sections (20 μm) using a sliding microtome (Model 2010-17, Shanghai Medical Instrument Corp., Shanghai, China). We stained the stem cross-sections with safranin and astra-blue, rinsed them in water, and mounted them onto slides. We observed the samples under a compound microscope (Leica ICC50, Wetzlar, Germany) and took images under a magnification of 10× with a built-in digital camera for analysis in ImageJ. We calculated mean vessel diameter (μm) assuming a circular shape, and vessel density (VD, no. mm^{-2}) as the number of vessels per xylem area on randomly chosen sectors from each cross-section. We calculated the mean hydraulically weighted xylem vessel diameter (D_h, μm) on the basis of vessel contribution to hydraulic conductance according to the following equation: $\Sigma d^5/\Sigma d^4$ [50], where d = vessel diameter.

We obtained the data on functional traits, including percentage loss of hydraulic conductance (PLC) data, at the lowest elevational site (*deciduous broadleaf 1*; 735 m altitude) from our previous study [51]. By combining these data with those of the present study, we can test the hypothesis that a large conduit diameter leads to high sensitivity to freeze-thaw-induced embolism in winter (Figure S1). Although it would have been ideal to collect PLC at all the sites, we were unable to do so for the present study due to access difficulties arising from frequent storms and snow in winter.

2.4. Climate Variables

We used temperature and precipitation variables to quantify climate conditions at each site, including two temperature variables (mean annual temperature, mean temperature of the coldest quarter), and two precipitation variables (annual precipitation, precipitation of the driest quarter). We obtained all data from the 1-km spatial resolution (~ 30 s) WorldClim Version 2 database (worldclim.org), which are appropriate to describe the conditions on steep mountainsides [44]. All variables represent the average values over 30 years from 1970 to 2000.

2.5. Statistical Analysis

To test relationships between species mean values in functional traits and upper limit of species distributions, between elevations and climatic variables, we fit bivariate relationships using parametric coefficients (r^2) and *P*-values (*P*), and fit lines by using linear regression or nonlinear curve fitting (SigmaPlot v12.5, Systat Software, Inc., San Jose, CA, USA). For the two congeneric species pairs (*Betula ermanii* and *B. platyphylla*, *Alnus mandshurica* and *A. japonica*), we did Student *t*-tests with the mean species values to test the interspecific differences within each species pair. Prior to any statistical analysis, we tested all functional traits for normality and $\log_{10}$-transformed them to improve normality if they were not normally distributed.

Given that multiple species unevenly across the elevational gradient due to upper distributional limits, we designed a series of general linear mixed-effects models implemented using the `lme4` library [52] in the R statistical and programming language [53], setting each trait of interest as the response and species as the random effect. Our main hypothesis was that there was an elevational shift in the values of each trait, but not necessarily a linear one. We therefore contrasted three simple models for each trait: (1) a second-order polynomial of elevation, (2) a linear change with elevation, and (3) and intercept-only model (separate intercepts per species). We compared the relative probability of each model in the trait-specific model set using Akaike's information criterion corrected for small sample size (AIC_c) [54]. The bias-corrected relative weight of evidence for each model, given the data and the suite of candidate models considered, was the AIC_c weight; the smaller the weight, the lower its relative probability [54]. We also calculated the marginal R^2 of each resampled GLMM (R_m) as a measure of goodness of fit and the contribution of the fixed effects to explaining variance in the response variable [55]. We also repeated the analyses above using precipitation in the driest quarter instead of elevation as the predictor variable given it had the lowest correlation among all climate variables and elevation (results not shown). In cases where there was information-theoretic evidence for a change in the functional trait and elevation (see Results), we used the top-ranked model to predict a mean trait value across species to their putative upper elevational limit.

3. Results

There was a strong correlation (Pearson's $|r| > 0.81$) among all climate variables and elevation (Figure 2; Table S1), suggesting that elevation alone was a good proxy for the climate characteristics at all sites. Temperature (both mean annual and of the coldest quarter) declined quasi-linearly with rising elevation, and precipitation (annual and of the driest quarter) increased with increasing elevation (Figure 2a–c). However, the lowest correlations were for precipitation of the driest quarter (Figure 2d).

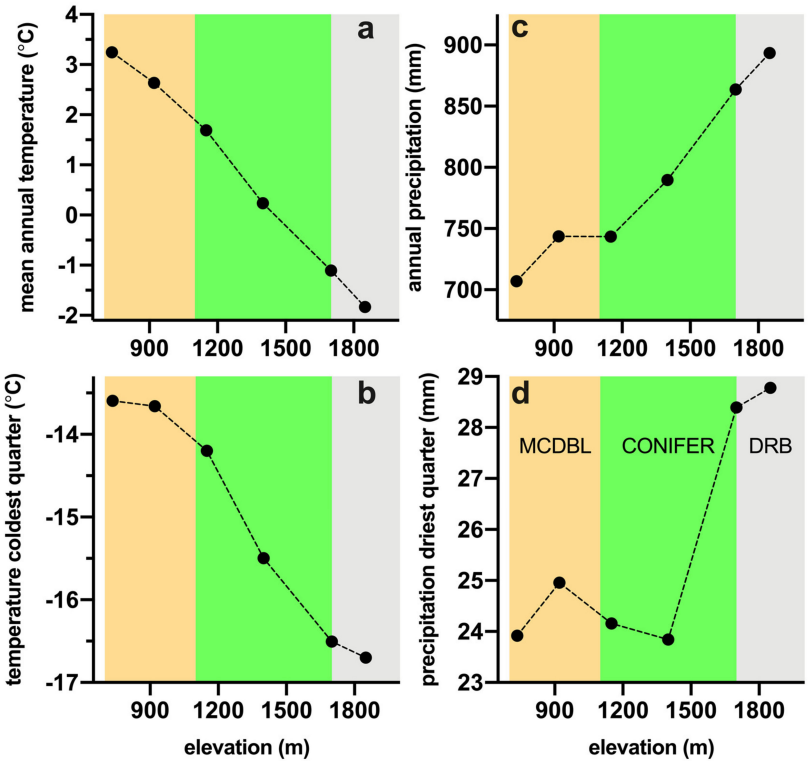

Figure 2. Trends in climatic variables of sampling sites along elevation: (**a**) mean annual temperature (°C), (**b**) temperature of the coldest quarter (°C), (**c**) annual precipitation (mm), and (**d**) precipitation of the driest quarter (mm). Also shown are the approximate elevational bands of the three main forest types sampled: MCDBL = mixed conifer-deciduous broadleaf (peach); CONIFER = conifer (green); DRB = dwarf rock birch (grey).

The interspecific coefficients of variation (CV) were 0.53, 0.67 and 0.16 for hydraulically weighted vessel diameter (D_h), vessel density (VD) and sapwood density (WD), respectively, among all these species (Table 3). Intraspecific variation was much lower than interspecific variation. For example, the highest CV of D_h was only 0.22 among the 10 species sampled (Table 3). Overall, the D_h was negatively related to upper limit of species distributions ($r^2 = 0.49$, $P = 0.025$; Figure 3a). We found no relationship between D_h and the upper limit when only the seven diffuse-porous species were analyzed. We found no evidence for correlations between xylem vessel density and UL, or between sapwood density and UL across all 10 species (Figure 3b,c). The three ring-porous species FM (*Maackia amurensis*), MA (*Maackia amurensis*) and PA (*Phellodendron amurense*) with the widest D_h had the lowest UL along elevations (Figure 3a). Sub-canopy species with the narrowest D_h had the highest UL, except for the two treeline species BE (*Betula ermanii*) and AM (*Alnus mandshurica*) with the highest elevational distributions. Moreover, the polynomial mixed-effects models predicted the mean trait values for D_h and VD for all species to their putative elevational limits (Figure S2 and Table S2).

Table 3. The mean values and intraspecific coefficients of variation (CV) for the three studied functional traits in the 10 temperate deciduous tree species studied along the altitudinal gradient. hydraulically weighted vessel diameter (D_h, μm), xylem vessel density (VD, mm^{-2}), and sapwood density (WD, $g\ cm^{-3}$). Species codes are given in Table 1.

Species	D_h		VD		WD	
	Mean	CV	Mean	CV	Mean	CV
FM	79.23	0.05	29.68	0.24	0.56	0.04
MA	59.42	0.14	54.54	0.09	0.51	0.08
PA	64.69	0.11	66.6	0.13	0.43	0.05
PU	31.57	0.04	352.44	0.1	0.46	0.07
TA	27.94	0.22	550.03	0.43	0.29	0.04
SP	22.58	0.05	644.29	0.17	0.48	0.09
BP	29.78	0.06	260.19	0.14	0.48	0.06
BE	35.99	0.08	129.68	0.2	0.52	0.09
AJ	26.42	0.12	395.09	0.27	0.38	0.05
AM	25.43	0.12	395.16	0.28	0.42	0.1
Total	37.87	0.53	327.7	0.67	0.45	0.16

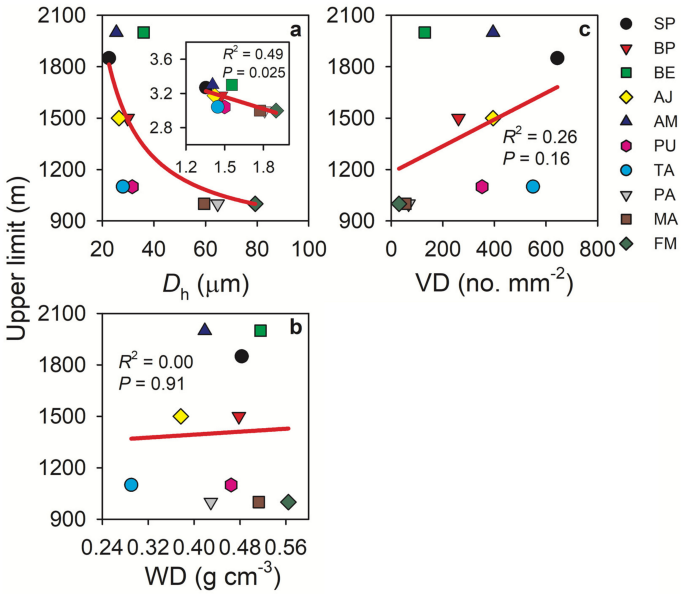

Figure 3. Relationships between upper limit UL of 10 species studied and hydraulically weighted vessel diameter D_h (**a**), stem sapwood density WD (**b**), and xylem vessel density VD (**c**). In panel (**a**), the inset figure shows the same relationships on a log–log scale. Symbols show species mean values (n = 6). AJ = *Alnus japonica*; AM = *Alnus mandshurica*; BE = *Betula ermanii*; BP = *Betula platyphylla*; FM = *Fraxinus mandshurica*; MA = *Maackia amurensis*; PA = *Phellodendron amurense*; PU = *Populus ussuriensis*; SP = *Sorbus pohuashanensis*; TA = *Tilia amurensis*.

For the two treeline species, we observed some interesting phenomena within specific genera. For example, *Betula ermanii* from higher elevations had higher D_h and WD and lower VD than *Betula platyphylla* from lower elevations (Figure S3). Similarly, *Alnus mandshurica* had higher D_h and WD at high elevations than *Alnus japonica* at lower elevations (Figure S4). In addition, both *Betula ermanii* and *Alnus mandshurica* (the two treeline species) had a higher distributional upper limit than their lower elevation congeneric species, i.e., *Betula platyphylla* and *Alnus japonica*.

The general linear mixed-effects models revealed a non-linear (second-order polynomial) effect for D_h and VD except for WD (Table 4; Figure 4). For sapwood density, while there was some support for the polynomial model, it explained only a small component (0.6%) of the variation in the trait values (Table 4).

Table 4. Information-theoretic ranking of candidate models for each of the three functional traits tested: (**a**) hydraulically weighted vessel diameter, (**b**) vessel density, and (**c**) sapwood density. Shown are the three models contrasted per trait, where elevation (*elev*) is applied as a second-order polynomial, a linear change, or no relationship (intercept-only model). All models include a random species effect (1|*spp*). Also shown for each model are the log-likelihoods (LL), number of estimated model parameters (*k*), the difference in Akaike's information criterion (corrected for small samples) between the current and top ranked model (ΔAIC_c), the model probability ($wAIC_c$), and the marginal R^2 (R_m; contribution of fixed effects to the total variance explained by the model).

Trait/Model	LL	*k*	ΔAIC_c	$wAIC_c$	R_m
(a) hydraulically weighted vessel diameter					
~ *elev* + *elev*^{2} + 1|*spp*	208.5	5	-	0.997	1.6
~ *elev* + 1|*spp*	195.6	4	11.7	0.003	1.4
~ 1|*spp*	199.2	3	22.8	<0.001	-
(b) vessel density					
~ *elev* + *elev*^{2} + 1|*spp*	−119.1	5	-	0.998	3.2
~ *elev* + 1|*spp*	−135.4	4	13.0	0.001	1.3
~ 1|*spp*	−129.5	3	14.3	<0.001	-
(c) sapwood density					
~ 1|*spp*	229.0	3	-	0.444	-
~ *elev* + *elev*^{2} + 1|*spp*	226.6	5	0.3	0.392	0.6
~ *elev* + 1|*spp*	218.8	4	2.0	0.164	<0.1

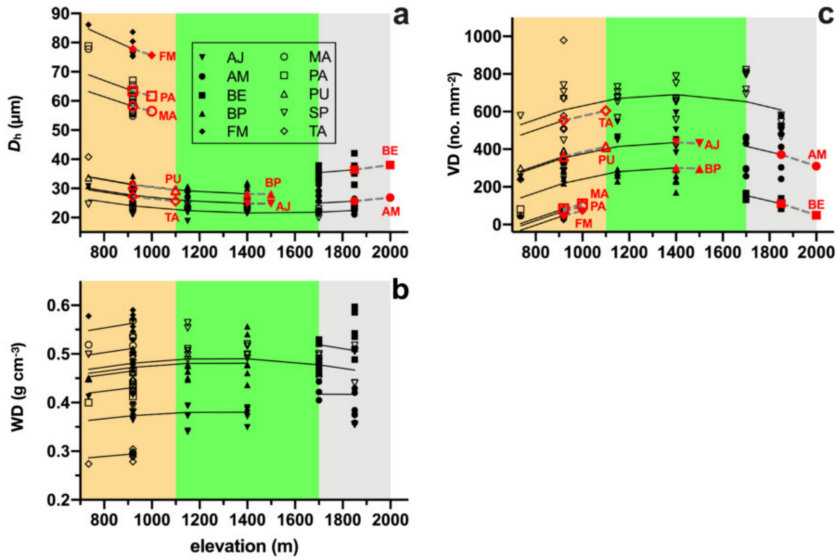

Figure 4. Change in functional traits relative to elevation for 10 species. (**a**) Hydraulically weighted vessel diameter (D_h, µm) initially decreased with increasing elevation, then stabilized and rose again at higher elevations (however, the variance explained was low; see Table 2). (**b**) There was no evidence that stem sapwood density (WD, g cm^{-3}) changed with elevation. Predicted trait values at their putative upper elevational limits are shown in red (values provided in Table S2 and Figure 4). No prediction was made for sapwood density given the lack of evidence for an effect of elevation. (**c**) There was evidence for a peak in vessel density (VD, mm^2) at mid-range latitudes. Also shown in each panel are the approximate elevational bands of the three main forest types sampled: MCDBL = mixed conifer-deciduous broadleaf (peach); CONIFER = conifer (green); DRB = dwarf rock birch (grey).

4. Discussion

Our results show that hydraulically weighted vessel diameter (D_h) declined with elevation for most of the tree species examined along the elevational gradient, but only in the lower-elevation forest

bands (mixed conifer-deciduous broadleaf and conifer forests). At least for the low- and mid-elevation species, variation in xylem structures appears to explain the trees' upper distributional limits. Similar results have been found elsewhere, including in Hawai'i where the tree *Metrosideros polymorpha* had consistently smaller D_h in subalpine habitats that experience freezing than in lowland rain forest habitats [56]. Likewise, *Larrea* species growing at high latitudes in America had a higher frequency of smaller vessels than plants growing at lower latitudes, suggesting increased protection from freeze-thaw embolism [57]. Xylem conduits are prone to embolism induced by frequent freeze-thaw events in winter, with a negative influence on xylem function [43]. Indeed, conduit diameter was proportional to the percentage loss of xylem conductivity after freezing [58–60] since wide conduits face higher risks of freeze-thaw-induced embolism [44].

We found evidence for a positive correlation between hydraulically weighted vessel diameter and degrees of xylem embolism during winter (see Figure S1). This suggests that freezing-induced loss of hydraulic conductivity over winter can be an important limiting factor for distributional limits of tree species in temperate regions [15,40,42], although some studies have showed that growing season temperatures and length also have strong influences on plant distribution along elevational gradient [16,18]. Consistently, the ring-porous tree species (e.g., *Fraxinus mandshurica*, *Maackia amurensis*, and *Phellodendron amurense*) with the widest xylem vessels had the lowest distributional upper limits (Figure 3a), likely due to their greater sensitivity to the negative impact on xylem functions of more stressful environments at higher elevations. In particular, the large earlywood vessels of ring-porous species are highly vulnerable to cavitation by freezing, and these species lose a high proportion of stem hydraulic conductivity in winter [51,61]. In contrast, diffuse-porous species with small vessel diameter have less-efficient water transport [51,62], but these species with narrower xylem vessels have lower probabilities of freeze-thaw-induced embolism [62–64]. Although limited by diffuse-porous woody structure and low water transport, these diffuse-porous species have stronger cold tolerance (e.g., freeze/thaw-induced embolism) that contributes to higher elevational upper limits.

However, there was a no evidence for a relationship between D_h and UL among these seven diffuse-porous species and D_h hardly changed along altitude with much lower variation within species. This suggested that D_h is not an informative trait limiting altitude distribution for diffuse-porous tree species. Previous results have shown that vessel diameters <44 μm represent a fine-tuning adaptation in avoiding freezing-induced embolism [44,60]. In fact, D_h values of all the seven studied diffuse-porous species fell well below this threshold, which might be responsible for low variation in vessel diameter in response to elevation change in these species [60]. The conservative xylem characteristics favouring tree adaptation in cold environments have also been found within species or genera [65], which could uncouple xylem traits from other climatic drivers along elevational gradients, e.g., precipitation. Vessel diameter did not show a clear pattern of change with precipitation (Table S3), indicating a weak influence of precipitation on plant hydraulic functionality in the present study site. Sapwood density (WD) with low intraspecific variation was not related to elevation, although variation in WD is generally accepted in terms of potentially explaining altitudinal limits of species [66].

Unexpectedly, the two treeline species *Betula ermanii* and *Alnus mandshurica* had larger D_h at higher elevations than their low-elevation congeneric, i.e., *B. platyphylla* and *A. japonica*. Although wider conduits are more vulnerable to embolism induced by frost and freeze-thaw events, the mean vessel diameters of *Betula ermanii* and *Alnus mandshurica* (30.97 μm and 23.20 μm, respectively) having highest upper-limit distribution (Figure 4a) were not near the critical threshold (44 μm) of purported catastrophic xylem dysfunction in environments with freeze-thaw stress [44]. This could indicate a low probability of catastrophic hydraulic failures for these two species, even though they occur at the highest elevations. Additionally, other hydraulic safety mechanisms could contribute to their adaptation at higher elevations. Tree species at higher elevations need to cope with both frost and physiological drought from lower winter temperatures and more frequent storms [47], because freeze-thaw cycles and winter desiccation at subalpine timberline habitats can threaten the integrity of stem hydraulic function [60,67,68]. Previous research has shown that *Betula ermanii* at higher elevations has more

negative water potentials corresponding to 50% loss of stem hydraulic conductivities and higher resistance to drought-induced embolism compared to *B. platyphylla*, despite it having larger vessel diameters than the latter species [27]. Vessel characteristics other than diameter (e.g., pit traits) can also play important roles in determining xylem hydraulic safety [27,62,69]. There is evidence that *Betula ermanii* has narrower and more elliptical pit apertures and hence, greater resistance to embolism propagation than the congeneric *B. platyphylla* in terms of pit-level anatomical traits [27]. Thus, these multiple hydraulic-safety strategies guaranteed by both xylem tissue level and pit level characteristics can potentially facilitate colonization of these two treeline species at the highest elevations.

5. Conclusions

Our study show that measurements of the variation in xylem traits could contribute to a better understanding of the upper range of species distributions along the altitudinal gradient. In temperate forests, trees at low-elevation sites generally possess traits associated with high hydraulic efficiency (wider vessels), thereby contributing to higher leaf gas-exchange rates and hence, higher growth rates. In contrast, trees at high-elevation sites exhibit traits associated with greater resistance to freezing-induced xylem embolism (narrower vessels), enhancing hydraulic safety in overwintering organs. Our results highlight the need for introducing hydraulic traits into ecosystem models for predicting future tree-distribution patterns.

Supplementary Materials: The following are available online at http://www.mdpi.com/1999-4907/11/3/349/s1, Figures S1–S4: Figure S1. Mean values of D_h (hydraulically weighted vessel diameter) and PLC (percentage loss of hydraulic conductance induced by freeze/thaw events and frost in winter of eight tree species studied at 735 m in this study(a), and the relationship between D_h and PLC on a log–log scale (b); Figure S2. Predicted functional traits: (a) D_h; (b) vessel density VD values at each species' upper elevational limit derived from the top-ranked mixed-effects models; Figure S3. Comparisons of D_h (a), sapwood density WD (b), and VD (c) between *Betula platyphylla* (BP) and *Betula ermanii* (BE); Figure S4. Comparisons of D_h (a), WD (b), and VD (c) between *Alnus japonica* (AJ) and *Alnus mandshurica* (AM). Table S1–S3: Table S1. Pearson correlation matrix between elevation and four environmental variables; Table S2. Predicted functional trait (D_h and VD) values at each species' upper elevational limit derived from the top-ranked mixed-effects models; Table S3. Information-theoretic ranking of candidate models for each of the four functional traits tested: (a) D_h, (b) VD, and (c) WD. Supplementary data: The mean values for the three studied functional traits of ten studied species at each sampling site.

Author Contributions: D.Y. and G.-Y.H. conceived the ideas and designed the experiment; D.Y. and A.-Y.W. collected the data; D.Y., J.-L.Z. and C.J.A.B. analyzed the data; D.Y. and G.-Y.H. led the writing of the manuscript. All authors contributed critically to the manuscript revising and editing and gave final approval for publication. All authors have read and agreed to the published version of the manuscript.

Funding: This research was funded by the National Natural Science Foundation of China (31722013, 31870593, 31500222, 31901284), the National Key Research and Development Program of China (2016YFA0600803), the K. C. Wong Education Foundation, the Key Research Project from the Bureau of Frontier Science and Education (QYZDJSSW-DQC027, ZDBS-LY-DQC019) of Chinese Academy of Sciences, the Liaoning Revitalization Talents Program (XLYC1807204).

Conflicts of Interest: The authors declare no conflict of interest.

References

1. Chabot, B.F.; Billings, W.D. Origins and Ecology of the Sierran Alpine Flora and Vegetation. *Ecol. Monogr.* **1972**, *42*, 163–199. [CrossRef]
2. Kearney, M.R.; Porter, W. Mechanistic niche modelling: Combining physiological and spatial data to predict species' ranges. *Ecol. Lett.* **2009**, *12*, 334–350. [CrossRef] [PubMed]
3. Rueda, M.; Godoy, O.; Hawkins, B.A. Spatial and evolutionary parallelism between shade and drought tolerance explains the distributions of conifers in the conterminous United States. *Glob. Ecol. Biogeogr.* **2016**, *26*, 31–42. [CrossRef]
4. Valladares, F.; Niinemets, Ü. Shade Tolerance, a Key Plant Feature of Complex Nature and Consequences. *Annu. Rev. Ecol. Evol. Syst.* **2008**, *39*, 237–257. [CrossRef]

5. Martínez-Tillería, K.; Loayza, A.P.; Sandquist, D.R.; Squeo, F. No evidence of a trade-off between drought and shade tolerance in seedlings of six coastal desert shrub species in north-central Chile. *J. Veg. Sci.* **2012**, *23*, 1051–1061. [CrossRef]
6. Kunstler, G.; Falster, D.S.; Coomes, D.A.; Hui, F.; Kooyman, R.M.; Laughlin, D.C.; Poorter, L.; Vanderwel, M.; Vieilledent, G.; Wright, S.J.; et al. Plant functional traits have globally consistent effects on competition. *Nature* **2015**, *529*, 204–207. [CrossRef]
7. Elith, J.; Graham, C.H.; Anderson, R.P.; Dudík, M.; Ferrier, S.; Guisan, A.; Hijmans, R.J.; Huettmann, F.; Leathwick, J.R.; Lehmann, A.; et al. Novel methods improve prediction of species' distributions from occurrence data. *Ecography* **2006**, *29*, 129–151. [CrossRef]
8. Figueroa, J.A.; Cabrera, H.M.; Queirolo, C.; Hinojosa, L.F. Variability of water relations and photosynthesis in Eucryphia cordifolia Cav. (Cunoniaceae) over the range of its latitudinal and altitudinal distribution in Chile. *Tree Physiol.* **2010**, *30*, 574–585. [CrossRef]
9. Swaine, M.D. Rainfall and Soil Fertility as Factors Limiting Forest Species Distributions in Ghana. *J. Ecol.* **1996**, *84*, 419. [CrossRef]
10. Engelbrecht, B.M.J.; Comita, L.; Condit, R.; Kursar, T.A.; Tyree, M.T.; Turner, B.L.; Hubbell, S.P. Drought sensitivity shapes species distribution patterns in tropical forests. *Nature* **2007**, *447*, 80–82. [CrossRef]
11. Baltzer, J.L.; Davies, S.J.; Bunyavejchewin, S.; Noor, N.S.M. The role of desiccation tolerance in determining tree species distributions along the Malay–Thai Peninsula. *Funct. Ecol.* **2008**, *22*, 221–231. [CrossRef]
12. Guisan, A.; Zimmermann, N.E. Predictive habitat distribution models in ecology. *Ecol. Model.* **2000**, *135*, 147–186. [CrossRef]
13. Higgins, S.I.; O'Hara, R.B.; Römermann, C. A niche for biology in species distribution models. *J. Biogeogr.* **2012**, *39*, 2091–2095. [CrossRef]
14. Svenning, J.-C.; Sandel, B. Disequilibrium vegetation dynamics under future climate change. *Am. J. Bot.* **2013**, *100*, 1266–1286. [CrossRef]
15. Sakai, A.; Weiser, C.J. Freezing Resistance of Trees in North America with Reference to Tree Regions. *Ecology* **1973**, *54*, 118–126. [CrossRef]
16. Normand, S.; Treier, U.A.; Randin, C.; Vittoz, P.; Guisan, A.; Svenning, J.-C. Importance of abiotic stress as a range-limit determinant for European plants: Insights from species responses to climatic gradients. *Glob. Ecol. Biogeogr.* **2009**, *18*, 437–449. [CrossRef]
17. Mellert, K.H.; Fensterer, V.; Küchenhoff, H.; Reger, B.; Kolling, C.; Klemmt, H.J.; Ewald, J. Hypothesis-driven species distribution models for tree species in the Bavarian Alps. *J. Veg. Sci.* **2011**, *22*, 635–646. [CrossRef]
18. Siefert, A.; Lesser, M.R.; Fridley, J.D. How do climate and dispersal traits limit ranges of tree species along latitudinal and elevational gradients? *GloB. Ecol. Biogeogr.* **2015**, *24*, 581–593. [CrossRef]
19. Körner, C.; Paulsen, J. A world-wide study of high altitude treeline temperatures. *J. Biogeogr.* **2004**, *31*, 713–732. [CrossRef]
20. Adler, P.B.; Salguero-Gómez, R.; Compagnoni, A.; Hsu, J.S.; Ray-Mukherjee, J.; Mbeau-Ache, C.; Franco, M. Functional traits explain variation in plant life history strategies. *Proc. Natl. Acad. Sci. USA* **2013**, *111*, 740–745. [CrossRef]
21. Reich, P.B. The world-wide 'fast-slow' plant economics spectrum: A traits manifesto. *J. Ecol.* **2014**, *102*, 275–301. [CrossRef]
22. Salgado-Negret, B.; Canessa, R.; Valladares, F.; Armesto, J.J.; Pérez, F. Functional traits variation explains the distribution of Aextoxicon punctatum (Aextoxicaceae) in pronounced moisture gradients within fog-dependent forest fragments. *Front. Plant Sci.* **2015**, *6*, 511. [CrossRef] [PubMed]
23. Saura, J.M.C.; Martínez-Vilalta, J.; Trabucco, A.; Spano, D.; Mereu, S. Specific leaf area and hydraulic traits explain niche segregation along an aridity gradient in Mediterranean woody species. *Perspect. Plant Ecol. Evol. Syst.* **2016**, *21*, 23–30. [CrossRef]
24. Díaz, S.; Cabido, M. Vive la différence: Plant functional diversity matters to ecosystem processes. *Trends Ecol. Evol.* **2001**, *16*, 646–655. [CrossRef]
25. McGill, B.; Enquist, B.J.; Weiher, E.; Westoby, M. Rebuilding community ecology from functional traits. *Trends Ecol. Evol.* **2006**, *21*, 178–185. [CrossRef] [PubMed]
26. Westoby, M.; Wright, I.J. Land-plant ecology on the basis of functional traits. *Trends Ecol. Evol.* **2006**, *21*, 261–268. [CrossRef] [PubMed]

27. Zhang, W.-W.; Song, J.; Wang, M.; Liu, Y.-Y.; Li, N.; Zhang, Y.; Holbrook, N.M.; Hao, G.-Y. Divergences in hydraulic architecture form an important basis for niche differentiation between diploid and polyploid Betula species in NE China. *Tree Physiol.* **2017**, *37*, 604–616. [CrossRef]
28. Brodribb, T.J.; Hill, R.S. The importance of xylem constraints in the distribution of conifer species. *New Phytol.* **1999**, *143*, 365–372. [CrossRef]
29. Cavender-Bares, J.; Holbrook, N.M. Hydraulic properties and freezing-induced cavitation in sympatric evergreen and deciduous oaks with contrasting habitats. *Plant, Cell Environ.* **2001**, *24*, 1243–1256. [CrossRef]
30. Choat, B.; Sack, L.; Holbrook, N.M. Diversity of hydraulic traits in nine Cordia species growing in tropical forests with contrasting precipitation. *New Phytol.* **2007**, *175*, 686–698. [CrossRef]
31. Brodribb, T.J.; Bowman, D.J.M.S.; Nichols, S.; Delzon, S.; Burlett, R. Xylem function and growth rate interact to determine recovery rates after exposure to extreme water deficit. *New Phytol.* **2010**, *188*, 533–542. [CrossRef] [PubMed]
32. Markesteijn, L.; Poorter, L.; Paz, H.; Sack, L.; Bongers, F. Ecological differentiation in xylem cavitation resistance is associated with stem and leaf structural traits. *Plant, Cell Environ.* **2010**, *34*, 137–148. [CrossRef] [PubMed]
33. Bucci, S.J.; Scholz, F.G.; Campanello, P.I.; Montti, L.; Jiménez-Castillo, M.; Rockwell, F.A.; Manna, L.L.; Guerra, P.; Bernal, P.L.; Troncoso, O.; et al. Hydraulic differences along the water transport system of South American Nothofagus species: Do leaves protect the stem functionality? *Tree Physiol.* **2012**, *32*, 880–893. [CrossRef] [PubMed]
34. Tyree, M.T.; Sperry, J.S. Vulnerability of xylem to cavitation and embolism. *Annu. Rev. Plant Biol.* **1989**, *40*, 19–36. [CrossRef]
35. Zwieniecki, M.A.; Secchi, F. Threats to xylem hydraulic function of trees under 'new climate normal' conditions. *Plant Cell Environ.* **2014**, *38*, 1713–1724. [CrossRef]
36. Choat, B.; Jansen, S.; Brodribb, T.J.; Cochard, H.; Delzon, S.; Bhaskar, R.; Bucci, S.J.; Feild, T.S.; Gleason, S.M.; Hacke, U.; et al. Global convergence in the vulnerability of forests to drought. *Nature* **2012**, *491*, 752–755. [CrossRef]
37. Barigah, T.S.; Charrier, O.; Douris, M.; Bonhomme, M.; Herbette, S.; Ameglio, T.; Fichot, R.; Brignolas, F.; Cochard, H. Water stress-induced xylem hydraulic failure is a causal factor of tree mortality in beech and poplar. *Ann. Bot.* **2013**, *112*, 1431–1437. [CrossRef]
38. Tyree, M.T.; Zimmermann, M.H.; Tyree, P.M.T. *Xylem Structure and the Ascent of Sap*; Springer Science and Business Media LLC: Berlin/Heidelberg, Germany, 2002; pp. 27–48.
39. Fu, P.-L.; Jiang, Y.-J.; Wang, A.-Y.; Brodribb, T.J.; Zhang, J.-L.; Zhu, S.-D.; Cao, K.-F. Stem hydraulic traits and leaf water-stress tolerance are co-ordinated with the leaf phenology of angiosperm trees in an Asian tropical dry karst forest. *Ann. Bot.* **2012**, *110*, 189–199. [CrossRef]
40. Qian, H.; Hao, Z.; Zhang, J. Phylogenetic structure and phylogenetic diversity of angiosperm assemblages in forests along an elevational gradient in Changbaishan, China. *J. Plant Ecol.* **2014**, *7*, 154–165. [CrossRef]
41. Cobb, A.R.; Choat, B.; Holbrook, N.M. Dynamics of freeze-thaw embolism in Smilax rotundifolia (Smilacaceae). *Am. J. Bot.* **2007**, *94*, 640–649. [CrossRef]
42. Körner, C.; Basler, D.; Hoch, G.; Kollas, C.; Lenz, A.; Randin, C.F.; Vitasse, Y.; Zimmermann, N.E. Where, why and how? Explaining the low temperature range limits of temperate tree species. *J. Ecol.* **2016**, *104*, 1076–1088. [CrossRef]
43. Tyree, M.T.; Davis, S.D.; Cochard, H. Biophysical Perspectives of Xylem Evolution: Is there a Tradeoff of Hydraulic Efficiency for Vulnerability to Dysfunction? *IAWA J.* **1994**, *15*, 335–360. [CrossRef]
44. Davis, S.D.; Sperry, J.S.; Hacke, U. The relationship between xylem conduit diameter and cavitation caused by freezing. *Am. J. Bot.* **1999**, *86*, 1367–1372. [CrossRef] [PubMed]
45. Wu, G.; Jiang, P.; Wei, J.; Shao, H. Nutrients and biomass spatial patterns in alpine tundra ecosystem on Changbai Mountains, Northeast China. *Coll. Surf. B Biointerf.* **2007**, *60*, 250–257. [CrossRef]
46. Dai, L.; Qi, L.; Wang, Q.-W.; Su, D.; Yu, D.; Wang, Y.; Ye, Y.; Jiang, S.; Zhao, W. Changes in forest structure and composition on Changbai Mountain in Northeast China. *Ann. For. Sci.* **2011**, *68*, 889–897. [CrossRef]
47. Liu, Q.-J. Structure and dynamics of the subalpine coniferous forest on Changbai mountain, China. *Plant Ecol.* **1997**, *132*, 97–105. [CrossRef]

48. Xu, Z.; Yu, G.; Zhang, X.; Ge, J.; He, N.; Wang, Q.; Wang, D. The variations in soil microbial communities, enzyme activities and their relationships with soil organic matter decomposition along the northern slope of Changbai Mountain. *Appl. Soil Ecol.* **2015**, *86*, 19–29. [CrossRef]
49. Wang, D.; He, N.; Wang, Q.; Lü, Y.; Wang, Q.; Xu, Z.; Zhu, J. Effects of Temperature and Moisture on Soil Organic Matter Decomposition Along Elevation Gradients on the Changbai Mountains, Northeast China. *Pedosphere* **2016**, *26*, 399–407. [CrossRef]
50. Vilagrosa, A.; Hernández, E.I.; Luis, V.C.; Cochard, H.; Pausas, J.G. Physiological differences explain the co-existence of different regeneration strategies in Mediterranean ecosystems. *New Phytol.* **2013**, *201*, 1277–1288. [CrossRef]
51. Niu, C.-Y.; Meinzer, F.; Hao, G.-Y. Divergence in strategies for coping with winter embolism among co-occurring temperate tree species: The role of positive xylem pressure, wood type and tree stature. *Funct. Ecol.* **2017**, *31*, 1550–1560. [CrossRef]
52. Bates, D.; Mächler, M.; Bolker, B.; Walker, S. Fitting Linear Mixed-Effects Models Using lme4. *J. Stat. Softw.* **2015**, *67*, 1–48. [CrossRef]
53. R Core Team. *R: A Language and Environment for Statistical Computing*; R Foundation for Statistical Computing: Vienna, Austria, 2018. Available online: www.R-project.org (accessed on 1 August 2019).
54. Guthery, F.S.; Burnham, K.P.; Anderson, D.R. Model Selection and Multimodel Inference: A Practical Information-Theoretic Approach. *J. Wildl. Manag.* **2003**, *67*, 655. [CrossRef]
55. Nakagawa, S.; Schielzeth, H. A general and simple method for obtaining R2 from generalized linear mixed?effects models. *Methods Ecol. Evol.* **2012**, *4*, 133–142. [CrossRef]
56. Fisher, J.B.; Goldstein, G.; Jones, T.J.; Cordell, S. Wood vessel diameter is related to elevation and genotype in the Hawaiian tree Metrosideros polymorpha (Myrtaceae). *Am. J. Bot.* **2007**, *94*, 709–715. [CrossRef] [PubMed]
57. Medeiros, J.S.; Pockman, W. Freezing regime and trade-offs with water transport efficiency generate variation in xylem structure across diploid populations of Larrea sp. (Zygophyllaceae). *Am. J. Bot.* **2014**, *101*, 598–607. [CrossRef] [PubMed]
58. Feild, T.S.; Brodribb, T.; Brodribb, T.J. Stem water transport and freeze-thaw xylem embolism in conifers and angiosperms in a Tasmanian treeline heath. *Oecologia* **2001**, *127*, 314–320. [CrossRef] [PubMed]
59. Cavender-Bares, J.; Cortes, P.; Rambal, S.; Joffre, R.; Miles, B.; Rocheteau, A. Summer and winter sensitivity of leaves and xylem to minimum freezing temperatures: A comparison of co-occurring Mediterranean oaks that differ in leaf lifespan. *New Phytol.* **2005**, *168*, 597–612. [CrossRef]
60. Schreiber, S.; Hacke, U.; Hamann, A. Variation of xylem vessel diameters across a climate gradient: Insight from a reciprocal transplant experiment with a widespread boreal tree. *Funct. Ecol.* **2015**, *29*, 1392–1401. [CrossRef]
61. Christman, M.A.; Sperry, J.; Smith, D. Rare pits, large vessels and extreme vulnerability to cavitation in a ring-porous tree species. *New Phytol.* **2011**, *193*, 713–720. [CrossRef]
62. Hacke, U.; Sperry, J.S. Functional and ecological xylem anatomy. *Perspect. Plant Ecol. Evol. Syst.* **2001**, *4*, 97–115. [CrossRef]
63. Sperry, J.S.; Nichols, K.L.; Sullivan, J.E.M.; Eastlack, S.E. Xylem Embolism in Ring-Porous, Diffuse-Porous, and Coniferous Trees of Northern Utah and Interior Alaska. *Ecol.* **1994**, *75*, 1736–1752. [CrossRef]
64. Sperry, J.S.; Sullivan, J.E.M.; Zhu, G.L.; Boyer, J.S. Xylem Embolism in Response to Freeze-Thaw Cycles and Water Stress in Ring-Porous, Diffuse-Porous, and Conifer Species. *Plant Physiol.* **1992**, *100*, 605–613. [CrossRef]
65. Jacobsen, A.; Pratt, R.B. Vulnerability to cavitation of central California Arctostaphylos (Ericaceae): A new analysis. *Oecologia* **2012**, *171*, 329–334. [CrossRef] [PubMed]
66. Carrasco, F.; Quezada, I.; Saldaña, A. Variation in traits related to water transport in Nothofagus dombeyi helps to explain its latitudinal distribution limit in the Chilean Andes. *Plant Ecol. Divers.* **2018**, *11*, 307–317. [CrossRef]
67. Mayr, S.; Wolfschwenger, M.; Bauer, H. Winter-drought induced embolism in Norway spruce (Picea abies) at the Alpine timberline. *Physiol. Plant.* **2002**, *115*, 74–80. [CrossRef]

68. Granda, E.; Scoffoni, C.; Rubio-Casal, A.E.; Sack, L.; Valladares, F. Leaf and stem physiological responses to summer and winter extremes of woody species across temperate ecosystems. *Oikos* **2014**, *123*, 1281–1290. [CrossRef]
69. Li, M.; Wu, Z.; Qin, L.; Meng, X. Extracting vegetation phenology metrics in Changbai Mountains using an improved logistic model. *Chin. Geogr. Sci.* **2011**, *21*, 304–311. [CrossRef]